

Slow True Polar Wander Around Varying Equatorial Axes Since 320 Ma

 Bram Vaes^{1,2}  and Douwe J. J. van Hinsbergen¹ 
¹Department of Earth Sciences, Utrecht University, Utrecht, The Netherlands, ²Department of Earth and Environmental Sciences, University of Milano-Bicocca, Milan, Italy

Peer Review The peer review history for this article is available as a PDF in the Supporting Information.

Key Points:

- New estimates of the magnitude and rate of true polar wander (TPW) during the last 320 million years
- TPW mostly occurred about two nearly orthogonal equatorial axes
- No evidence for fast ($>1^\circ/\text{Ma}$) TPW rotations of >10 Ma since 320 Ma

Supporting Information:

Supporting Information may be found in the online version of this article.

Correspondence to:

B. Vaes,
bram.vaes@unimib.it

Citation:

Vaes, B., & van Hinsbergen, D. J. J. (2025). Slow true polar wander around varying equatorial axes since 320 Ma. *AGU Advances*, 6, e2024AV001515. <https://doi.org/10.1029/2024AV001515>

Received 24 SEP 2024
Accepted 24 FEB 2025

Author Contributions:

Conceptualization: Bram Vaes, Douwe J. J. van Hinsbergen
Data curation: Bram Vaes
Formal analysis: Bram Vaes
Funding acquisition: Douwe J. J. van Hinsbergen
Investigation: Bram Vaes, Douwe J. J. van Hinsbergen
Methodology: Bram Vaes, Douwe J. J. van Hinsbergen
Software: Bram Vaes
Visualization: Bram Vaes
Writing – original draft: Bram Vaes
Writing – review & editing: Douwe J. J. van Hinsbergen

© 2025. The Author(s).

This is an open access article under the terms of the [Creative Commons Attribution License](https://creativecommons.org/licenses/by/4.0/), which permits use, distribution and reproduction in any medium, provided the original work is properly cited.

Abstract True polar wander (TPW), the rotation of the solid Earth relative to the spin axis, is driven by changes in the Earth's moment of inertia induced by mantle convection and may have influenced past climate and life. Long-term TPW is typically inferred from large polar shifts in paleomagnetic apparent polar wander paths or computed directly by rotating them in a mantle reference frame. However, most apparent polar wander paths do not incorporate uncertainties in paleomagnetic data, which may bias estimates of TPW. Here, we provide new quantitative estimates of TPW since 320 Ma by placing a recent global apparent polar wander path corrected for age bias and with improved uncertainty quantification in existing mantle reference frames. We find large amplitude ($>10^\circ$) but slow TPW rotations that predominantly occurred about two equatorial axes that are approximately orthogonal. During the Triassic and Jurassic, a $\sim 24^\circ$ TPW oscillation occurred about an axis at $\sim 15^\circ\text{W}$, close to the present-day TPW axis at $\sim 10^\circ\text{E}$. In contrast, the TPW axis was located at $\sim 85^\circ\text{E}$ during a smaller oscillation ($\sim 6\text{--}10^\circ$) over the past ~ 80 Ma, as well as between 260 and 320 Ma. We propose that these varying TPW axes reflect changes in the distribution and flux of subduction in the Tethyan and Pacific realms. We find no evidence for previously postulated fast ($>1^\circ/\text{Ma}$) TPW oscillations in the Cretaceous and Late Jurassic. Finally, we propose that calibrating mantle convection models against reconstructed TPW will improve our understanding of mantle dynamics and the drivers of TPW itself.

Plain Language Summary True polar wander is the rotation of the Earth's crust and mantle relative to the spin axis. On geological timescales, true polar wander (TPW) is caused by movements of heavier or lighter material in the mantle, such as sinking tectonic plates. To compensate for these movements, the Earth rebalances itself by a rotation around an axis located on the equator. These rotations change the position of all continents simultaneously, influencing their latitude and potentially climate and life. Additionally, the location of the axis and the speed of TPW can provide important insights on the structure and movement of material in the Earth's mantle. In this study, we calculated the magnitude, speed, and axis of TPW for the last 320 million years. Our results suggest that while the rotations were large ($>10^\circ$), they were relatively slow. True polar wander mainly occurred around two different equatorial axes: one close to the present-day axis and the other about 90° away. The changing axis may be caused by changes in the location and amount of sinking tectonic plates over time. Lastly, we propose that models of mantle convection could help us better understand the drivers of TPW.

1. Introduction

Determining the rate of convective motions of the Earth's mantle is key in deciphering the drivers of plate tectonics and volcanism but is notoriously difficult to quantify from kinematic observations alone. True polar wander (TPW) provides an avenue to kinematically constrain mantle convective processes. TPW is the rotation of the Earth's mantle and crust (i.e., the solid Earth) relative to the spin axis, such that the axis of maximum non-hydrostatic moment of inertia remains closely aligned with the spin axis. On geological timescales, TPW is driven by the redistribution of density anomalies within the Earth's mantle (Evans, 2003; Goldreich & Toomre, 1969), which include sinking subducted slabs or rising mantle plumes (Steinberger & Torsvik, 2010). TPW rotations occur, by definition, about an axis located in the equatorial plane, bringing excess masses toward the equator and mass deficits toward the geographic poles (Evans, 2003; Gold, 1955). The magnitude and rate of TPW are primarily controlled by the spatial distribution and magnitude of mass heterogeneities and by the viscosity of the mantle (e.g., Rose & Buffett, 2017; Spada et al., 1992; Tsai & Stevenson, 2007). Quantitative estimates of TPW therefore provide kinematic constraints on the structure, rheology, and dynamics of the Earth's mantle. The primary tool to quantify TPW is paleomagnetism (e.g., Besse et al., 2021). However, estimates of TPW obtained

through paleomagnetism vary significantly, and the magnitude and rate at which TPW occurred in the geological past are uncertain.

Long-term (≥ 5 Ma) TPW is often quantified using apparent polar wander paths, which track the motion of the time-averaged paleomagnetic pole, assumed to coincide with the Earth's spin axis, relative to a tectonic plate (e.g., Besse & Courtillot, 2002; Torsvik et al., 2008). Phanerozoic TPW rotations have been determined by identifying common rotations of major continents observed from paleomagnetic data (e.g., Jurdy & Van der Voo, 1974; Steinberger & Torsvik, 2008; Torsvik et al., 2012, 2014). This approach has yielded relatively slow ($< 1^\circ/\text{Ma}$) TPW rates, but large in amplitude (up to $> 20^\circ$ in the Paleozoic and Mesozoic; Torsvik et al., 2014). On the other hand, rapid shifts in the position of the paleomagnetic pole have also been interpreted as evidence for fast TPW ($> 1^\circ/\text{Ma}$). Proposed episodes of fast TPW include a short-lived episode at ~ 84 Ma (Gordon, 1983; Mitchell et al., 2021; Sager & Koppers, 2000), a $\sim 30\text{--}40^\circ$ polar shift during the Late Jurassic referred to as the “Jurassic monster polar shift” (e.g., Kent et al., 2015; Kent & Irving, 2010; Muttoni & Kent, 2019), a $\sim 50^\circ$ polar shift in the Ordovician-Silurian (Jing et al., 2022) as well as a $\sim 90^\circ$ degrees oscillation in the Ediacaran (e.g., Mitchell et al., 2011; Robert et al., 2017). The occurrence of such fast and large amplitude TPW events not only has large implications for the structure and dynamics of the Earth's interior but may also have had profound consequences for the biosphere, sea level, climate and the geodynamo (e.g., Biggin et al., 2012; Domeier et al., 2023; Evans, 2003; Jing et al., 2022; Muttoni et al., 2013; Muttoni et al., 2025; Raub et al., 2007; Wang & Mitchell, 2023). However, the existence of these fast TPW episodes requires high-resolution paleomagnetic data with small age uncertainties and therefore remains controversial: several recent studies have questioned whether these polar shifts truly represent rapid TPW or rather represent paleomagnetic artifacts, noise, or non-dipole behavior of the Earth's magnetic field (e.g., Cottrell et al., 2023; Domeier et al., 2023; Kulakov et al., 2021).

The most direct way to quantify the rate and magnitude of TPW is through the comparison of paleomagnetic reference frames derived from an APWP and mantle reference frames that estimate plate tectonic motions relative to the ambient mantle, such as a hotspot reference frame (e.g., Andrews, 1985; Besse & Courtillot, 2002; Doubrovine et al., 2012; Livermore et al., 1984). Placing an APWP in a mantle reference frame enables the construction of a TPW path (TPWP) that provides a direct estimate of the motion between the spin axis and “mean” solid Earth. However, the record of well-defined hotspot tracks has so far limited the reliable application of this approach to computing TPW back to the Early Cretaceous (~ 120 Ma; Doubrovine et al., 2012; Torsvik et al., 2008). Studies using the most recent hotspot reference frames obtained TPWPs that show slow ($< 1.0^\circ/\text{Ma}$) but significant (up to $10\text{--}20^\circ$ in magnitude) TPW back to Mesozoic times (e.g., Besse & Courtillot, 2002; Doubrovine et al., 2012).

A clear limitation of most published estimates of TPW is that they were obtained using conventional, pole-based apparent polar wander paths, in which spatial and temporal uncertainties in the underlying data were not incorporated (e.g., Besse & Courtillot, 2002; Torsvik et al., 2012). The recent global APWP of Vaes et al. (2023) is the first in which these sources of uncertainty were propagated. One of the key steps forward of that global APWP is that estimates of APW rates may now be corrected for temporal bias, by computing the “effective” age of the reference pole positions of the APWP from the age distribution of the paleomagnetic data used as input for those poles. Vaes et al. (2023) showed that observed peaks in APW rate that have previously been interpreted as phases of relatively rapid TPW, such as a spike between 110 and 100 Ma (Doubrovine et al., 2012; Steinberger & Torsvik, 2008; Torsvik et al., 2012), disappeared after correcting for the “effective” age difference between successive reference poles of the APWP.

Here, we derive new quantitative estimates of the magnitude, direction, and rate of TPW since 320 Ma by comparing the recent global APWP of Vaes et al. (2023) with previously published mantle reference frames. We first compute TPWPs that track the motion of the time-averaged paleomagnetic pole relative to the deep mantle for the last 120 Ma using mantle frames based on hotspots with different underlying assumptions (Doubrovine et al., 2012; Müller et al., 1993; Torsvik et al., 2008). Next, we compute TPW back to 320 Ma using a recent mantle reference frame of Müller et al. (2022) that is based on a set of tectonic “rules” and was computed for the last 1 Ga. We test previous observations that show that TPW was limited since the mid-Cretaceous and analyze whether the axis of TPW has remained approximately stable, as previously proposed, or whether TPW rotations occurred around changing equatorial axes since 320 Ma. Next, we re-assess whether fast polar shifts that were previously interpreted as phases of TPW may truly represent rapid TPW or rather may have resulted from noise induced by age uncertainty or the use of paleopole averages in determining polar wander. Finally, we discuss the

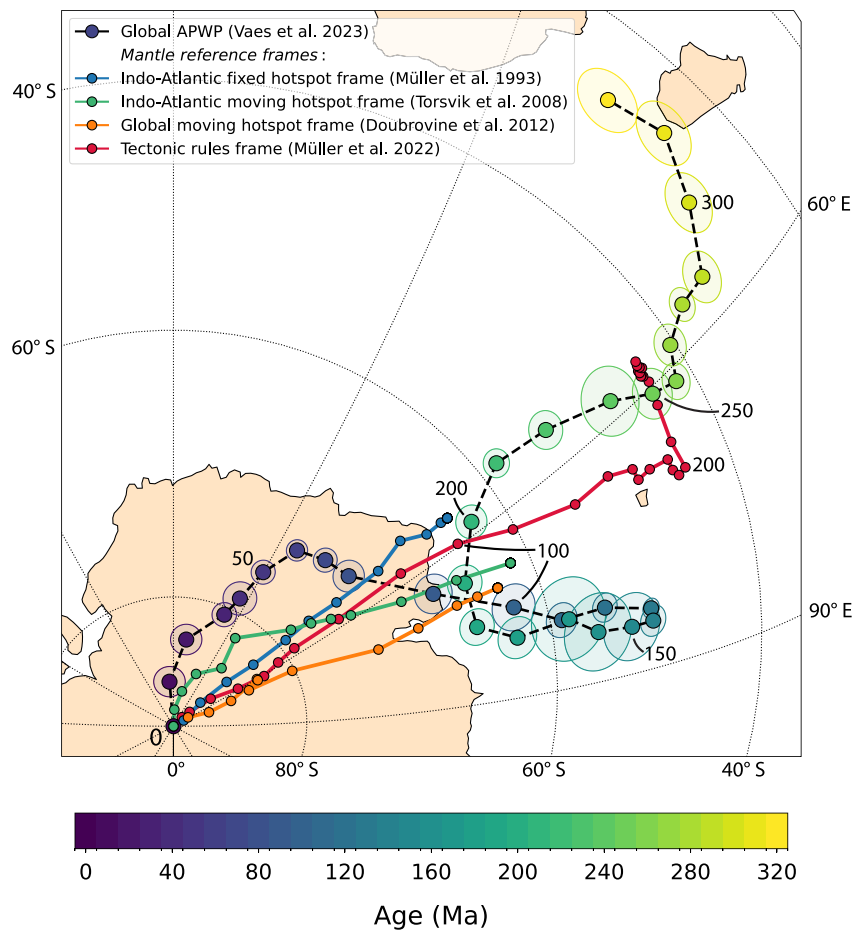


Figure 1. Comparison between the global APWP for the last 320 Ma of Vaes et al. (2023) and the four mantle reference frames used in this study to derive TPW. The global APWP is plotted in South African coordinates, thus showing the position of the Earth's spin axis relative to a fixed South Africa. The pole positions were computed at 10 Ma steps using a 20 Ma sliding window (Figure S1, Table S2 in Supporting Information S1). Reference poles and 95% confidence regions are colored by their age. The four polar wander paths constructed using the mantle reference frames indicate the motion the “mean” mantle relative to a fixed (South) African plate (Table S3 in Supporting Information S1). In the absence of TPW, this would correspond to the motion of the spin axis relative to the Africa plate. Note that these paths based on the mantle reference frames only go back to 120 Ma, except for the tectonic-rules-based frame of Müller et al. (2022), which is plotted here back to 320 Ma.

implications of our results for analyzing mantle dynamics and the role of deep-mantle structure in determining the axis of TPW.

2. Methods

We construct true polar wander paths using four different mantle reference frames (Figure 1, Table S1 in Supporting Information S1): the Indo-Atlantic fixed hotspot reference frame of Müller et al. (1993), the Indo-Atlantic moving hotspot reference frame of Torsvik et al. (2008), the global moving hotspot reference frame of Doubrovine et al. (2012), and the recently published mantle reference frame of Müller et al. (2022) that was constructed using a joint inversion approach constrained by a set of “tectonic rules” (Tetley et al., 2019). We computed each TPWP as an apparent polar wander path in a coordinate frame in which the mantle is kept fixed, following the approach of many previous workers (e.g., Andrews, 1985; Besse & Courtillot, 2002; Doubrovine et al., 2012; Livermore et al., 1984). To this end, we placed the recent global APWP of Vaes et al. (2023) in each of the mantle reference frames. We computed the TPWPs using a time step of 10 Ma, which is the temporal resolution at which both paleomagnetic and mantle reference frames are typically computed, as well as estimates

of TPW that are derived from those (e.g., Steinberger & Torsvik, 2008; Torsvik et al., 2014). To account for the uneven age distribution of the paleomagnetic input data, Vaes et al. (2023) computed the “effective” age of the reference poles and showed that this age is often significantly different from the center age of the 20 Ma time window used to compute each reference pole. To construct a global APWP at exact 10 Ma time steps, we re-computed the global APWP here using the same paleomagnetic database, global plate circuit and iterative approach used by Vaes et al. (2023). As an additional step, we interpolated between the reference poles generated for each iteration to obtain a cloud of simulated reference poles with the same age (e.g., 10, 20, 30 Ma; Figure S1 in Supporting Information S1). We emphasize that in this approach, both the spatial and temporal uncertainties in the underlying paleomagnetic data are propagated into the confidence regions of the global APWP. We quantify the 95% confidence regions of this interpolated APWP by the P_{95} cone of confidence, which includes 95% of the simulated reference poles computed for each time step, following the approach developed by Vaes et al. (2022, 2023) (Figure S1 in Supporting Information S1). Finally, to compute the TPWPs, we placed the interpolated global APWP in each mantle reference frame by rotating it using the Euler rotation poles (defined at 10 Ma steps) that describe the motion of the South African plate relative to the mantle. The resulting polar wander path then describes the motion of the time-averaged paleomagnetic pole relative to the ambient mantle, in the same way as a conventional APWP describes the motion of the pole relative to a fixed tectonic plate.

It is important to note that in our computation of the TPWP, the uncertainties associated with the mantle reference frames are not (yet) incorporated. The uncertainties of the rotation poles for Africa relative to the mantle were not quantified for the fixed hotspot reference frame of Müller et al. (1993) and the tectonic-rules-based frame of Müller et al. (2022). 95% confidence regions for the two moving hotspot reference frames were provided by Doubrovine et al. (2012) and Torsvik et al. (2008). In addition, we note that the plate circuit and time scale used to determine the mantle reference frames differs between all four models and is also different from the updated plate circuit as well as the time scale (of Gradstein et al., 2020) used for the construction of the global APWP of Vaes et al. (2023). Because the four reference frames are based on different input data sets, underlying assumptions, and methodologies, they each provide a different perspective on the motion of South Africa relative to the deep mantle.

The three hotspot-based mantle frames used here are assumed to determine the “absolute” motion of tectonic plates relative to the deep mantle using hotspot tracks: linear chains of intraplate volcanoes that show a clear progression of eruption ages (e.g., Morgan, 1971, 1981; Wilson, 1963). The geometry and age progression of these hotspot tracks have been widely used to reconstruct lithospheric motions relative to mantle upwellings (or “plumes,” Morgan, 1971), which are either assumed to be stationary in a “mean mantle” frame (i.e., a fixed hotspot reference frame, e.g., Morgan, 1981; Müller et al., 1993) or corrected for slow relative motions using a numerical model of mantle convection (i.e., a moving hotspot reference frame; Doubrovine et al., 2012; O’Neill et al., 2005; Torsvik et al., 2008). Moving hotspot reference frames, however, do not provide independent kinematic constraints on mantle dynamics because a mantle convection model, constrained by a global model of plate tectonic motions and mantle density heterogeneities, is used as input, after which the reference frame is iteratively constructed to fit hotspot tracks (e.g., Doubrovine et al., 2012; Torsvik et al., 2008). Moreover, constraining the relative motions between hotspots remains challenging. Wang et al. (2019) showed that the global moving hotspot reference frame of Doubrovine et al. (2012) provided worse fits to young (≤ 5 Ma) hotspot tracks compared to a frame in which hotspots are assumed to be fixed. Finally, it is worth noting that hotspot reference frames are limited by the availability of linear hotspot tracks, which only allows the determination of plate motions relative to hotspots back to the Early Cretaceous (~ 120 Ma).

The recent mantle reference frame of Müller et al. (2022) was constructed in an entirely different way. Building on the work of Tetley et al. (2019), they used an iterative approach in which the absolute plate motion of the reference plate Africa is obtained by a joint global inversion of absolute plate motions using four different criteria. These criteria include the restriction of the net lithospheric rotation rate to values deemed reasonable from numerical experiments, the minimization of global trench migration velocities, a global continental median plate velocity below 6.0 cm/a, and the minimization of the spatio-temporal misfit between observed and model-predicted hotspot tracks (only used for the last 80 Ma). We note that this type of mantle frame may be biased by subjective choices related to the relative weighting of the different rules and the imposed limits. On the other hand, the joint incorporation of multiple kinematic constraints enables the construction of a mantle frame that is less likely to suffer from errors in or the overfitting of a single kinematic observation such as a hotspot track (Tetley et al., 2019). Using the global plate model for the last billion years of Meredith et al. (2021) as input for

their model, Müller et al. (2022) constructed a tectonic-rules-based mantle reference frame since 1,000 Ma, using 5 Ma time steps. As with any plate reconstruction, their global plate model becomes increasingly more uncertain further back in geological time. The quantification of kinematic constraints like net lithospheric rotation and migration velocities of (intra-oceanic) trenches becomes particularly challenging for times prior to the Jurassic, from which no marine magnetic anomalies are preserved, which makes reconstructions of plate motions in regions like the Pacific-Panthalassa Ocean highly uncertain (e.g., Boschman et al., 2021). No attempts were made to quantify the uncertainties for the mantle frame of Müller et al. (2022), however. Nonetheless, taking this frame at face value enables, for the first time, the computation of a TPWP from 320 Ma to present, using the global APWP for the last 320 Ma of Vaes et al. (2023). Finally, to assess whether fast TPW phases may have occurred during the last 320 Ma, we also computed a TPWP at 5 Ma resolution, following the same procedure as described above, but using the 5-Ma-resolution-APWP (with a 10 Ma time window) of Vaes et al. (2023) instead.

3. Results

3.1. True Polar Wander Paths for the Last 120 Ma

We first computed four TPWPs for the last 120 Ma using the four different mantle reference frames (Figure 2, Table S3 in Supporting Information S1). The paths show the motion of the time-averaged paleomagnetic pole position, which is assumed to coincide with the spin axis, relative to the “mean” mantle. The TPWPs thus visualize the motion of the spin axis in a fixed mantle frame, providing direct estimates of the magnitude, rate, and direction of TPW. The four TPWPs show a similar first-order geometry for the last 120 Ma (Figures 2a–2d). All four paths show a back-and-forth motion of the spin axis during the last 80 Ma, roughly along the 180° meridian. From 80 to 60 Ma, all paths show a shift in the pole position away from the geographic pole (in a fixed mantle frame), with the net TPW angle peaking at 60 Ma in all four TPWPs. Notably low TPW rates of $<0.2^\circ/\text{Ma}$ are observed between ~60 and 20 Ma (Figure 2e) in all TPWPs, except for the TPWP based on the global moving hotspot reference frame of Doubrovine et al. (2012) for the interval between 40 and 60 Ma. This observed interval of insignificant TPW coincides with the mid-Cenozoic true polar “stillstand” proposed by Woodworth and Gordon (2018) based on a comparison between spin axis data and hotspots from the Pacific Ocean. The net angle of TPW of $>10^\circ$ at 60 Ma is notably larger for the Doubrovine et al. (2012) model than the $\sim 6^\circ$ for Müller et al. (1993) and Torsvik et al. (2008) models. The three TPW paths based on a hotspot reference frame show a sharp cusp at 80 Ma. Prior to 80 Ma, the trajectories of the TPWPs based on the Müller et al. (1993) and Doubrovine et al. (2012) frames are sub-parallel to the great circle around an equatorial TPW axis at 11°E , which is the proposed long-term TPW axis of Torsvik et al. (2014) that closely corresponds to the present-day axis of TPW and the geotectonic bipolarity axis (Pavoni, 2008). The TPWP computed using the Torsvik et al. (2008) frame shows a similar direction between 80 and 100 Ma but is perpendicular to this direction between 100 and 120 Ma. We observe very similar TPW rates for all four paths, consistent with previous results of Doubrovine et al. (2012) (Figure 2e). For most of the last 120 Ma, including the entire Cenozoic, the TPW rate is between $\sim 0.1^\circ/\text{Ma}$ and $0.4^\circ/\text{Ma}$. The highest TPW rates are obtained for the Late Cretaceous, peaking at a rate of $0.5\text{--}0.6^\circ/\text{Ma}$. Notably, we find that the TPW rate since 120 Ma—on a timescale of 10 Ma—stays well below $1.0^\circ/\text{Ma}$, which we defined as the threshold for “fast” TPW, following Cottrell et al. (2023).

3.2. A True Polar Wander Path Back to 320 Ma

We computed a TPWP back to 320 Ma by placing the interpolated global APWP of Vaes et al. (2023) in the tectonic-rules-based frame of Müller et al. (2022) (Figure 3, Table S4 in Supporting Information S1). The resulting TPWP can be roughly divided into five segments (Figure 4a). For the last 130 Ma, the TPW path shows an oscillatory motion with a cusp at 60 Ma. During this time interval, the path runs approximately parallel to the 5°W meridian, depicted in Figure 4a by the red line. The Jurassic-Triassic portion of the TPWP shows two smooth segments, from 130 to 200 Ma and from 200 to 260 Ma, that are nearly parallel. The trajectory corresponds to successive large TPW rotations around an equatorial axis located at $\sim 15^\circ\text{W}$ (blue line in Figure 4a). During both these time spans, the spin axis is estimated to move $\sim 24^\circ$ relative to the stable mantle. Note that the position of the spin axis relative to a fixed mantle is close to the present-day position at 260 and 250 Ma, just before the large back-and-forth TPW rotations. The oldest part of the TPWP, from 260 to 320 Ma, runs roughly parallel to the $5^\circ\text{W}/175^\circ\text{E}$ meridian, similar to the 0–130 Ma segments. The largest net TPW angle of approximately 21° is computed at 200 Ma and 320 Ma. The TPW rates computed for the last 320 Ma stay below $0.7^\circ/\text{Ma}$ for this entire time span, with an average of $0.34^\circ \pm 0.14^\circ/\text{Ma}$ (1σ).

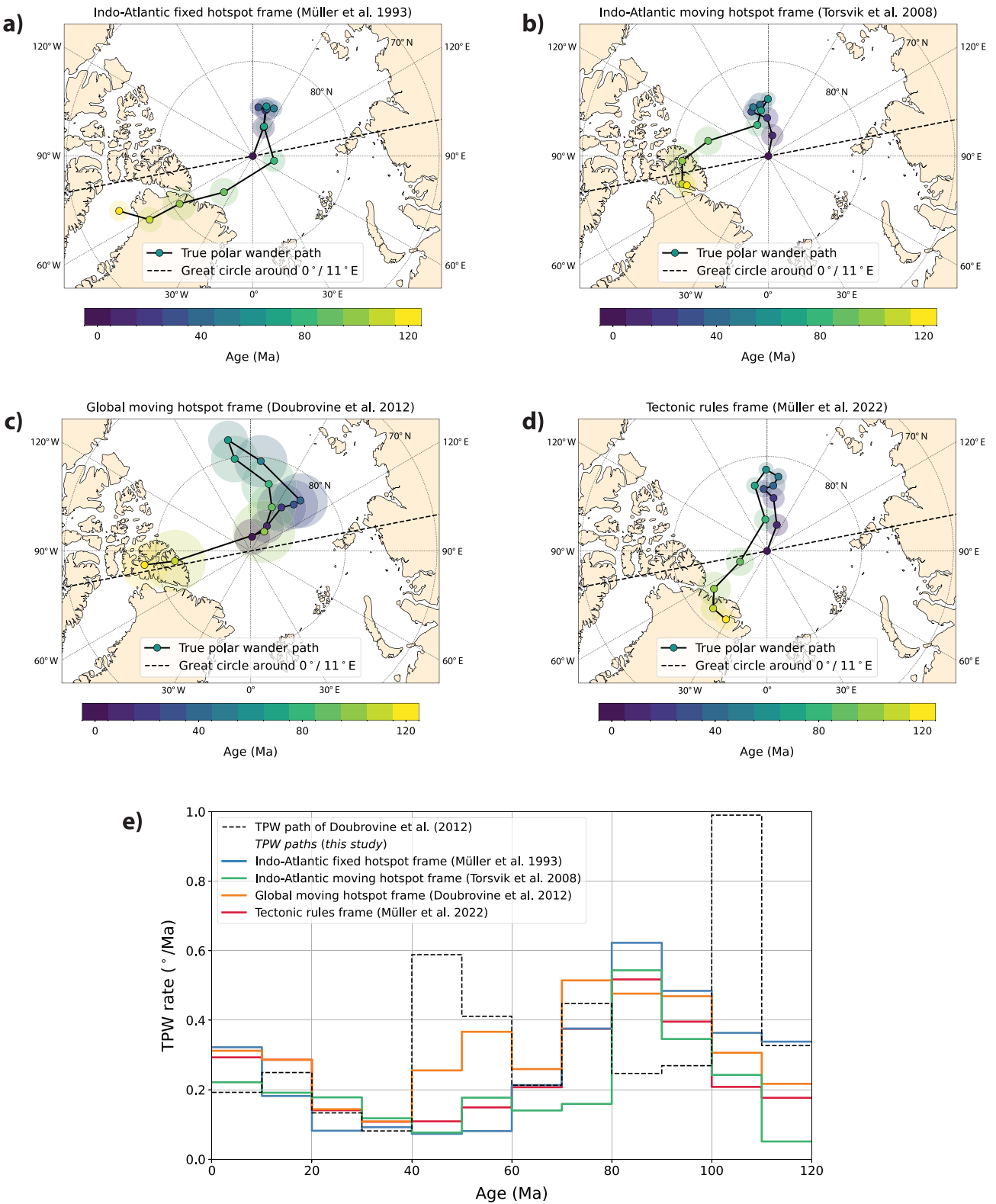


Figure 2.

The TPWP computed at 5 Ma resolution shows a similar overall trend but is more irregular and has much larger confidence regions (Figure 5, Table S5 in Supporting Information S1). Again, we emphasize that these confidence regions are solely defined by the uncertainty in the global APWP and do not incorporate those of the mantle reference frame—the true uncertainty must thus be larger. This is a direct consequence of the lower number of paleomagnetic data that underlies each pole position, given that a smaller time window of 10 Ma is used instead of 20 Ma. The main difference with the 10-Ma-resolution TPWP is that there are segments of the path showing a zig-zag pattern, for instance between 10 and 60 Ma (Figure 5a). However, whether these motions are truly representative of TPW is questionable considering the relatively large and often overlapping (minimum) confidence regions. Moreover, these confidence regions are based on the uncertainty in the global APWP only and therefore minimum estimates. The larger uncertainty is also clearly reflected in the confidence regions of the APW rate of the 5-Ma-resolution-APWP (Figure 5b). The TPW rates obtained from this higher resolution TPWP are ~50% higher than for the 10-Ma-resolution path, with a mean rate of $0.50^\circ \pm 0.27^\circ/\text{Ma}$ (Figure 5c). In addition, five peaks are observed with a TPW rate of $>0.8^\circ/\text{Ma}$, with three peaks above $1.0^\circ/\text{Ma}$. It should be noted, however, that the latter peaks are observed for the pre-260 Ma portion of the TPWPs, where the 5-Ma-resolution-APWP is the least robust and where the tectonic-plates-based mantle frame likely has higher uncertainty than for younger times.

4. Discussion

4.1. True Polar Wander Since 320 Ma

We have quantified the motion of the time-averaged paleomagnetic pole relative to the mantle using the global APWP of Vaes et al. (2023) and four different mantle reference frames. If these motions correspond to the movement of the Earth's spin axis relative to the mantle, they quantify the magnitude, rate, and direction of TPW. The similarities between the first-order geometry of the four TPWPs for the last 120 Ma indicates that the observed trends in polar motion are reproducible, even though these paths were constructed using mantle reference frames based on different data sets, plate circuits and approaches. Our results clearly show that TPW since 120 Ma is non-negligible: each TPWP yields an angular deviation of the spin axis relative to the mantle of $>5^\circ$ for both the early Cenozoic (50–60 Ma) and Early Cretaceous. This would argue for a rejection of the null hypothesis that no significant TPW occurred since the Late Cretaceous, in contrast to the conclusions reach in a recent paper by Cottrell et al. (2023) (Figure 4b). If the TPW rotations computed here are artifacts, this would imply a large and systematic error in either the global APWP or mantle reference frames. Given the well-constrained and small uncertainty of the global APWP of Vaes et al. (2023), this would suggest that there are large inadequacies in all mantle reference frames used here, for instance due to a large drift of all the hotspots or large, systematic errors in the relative plate motion circuit, which we consider unlikely.

The four TPWPs of the last 120 Ma all indicate a back-and-forth motion of the mantle relative to the spin axis during the last 80 Ma (Figures 2a–2d). This oscillatory motion was previously computed by Doubrovine et al. (2012) in a comparison of their moving hotspot frame and the global APWP of Torsvik et al. (2012). Intriguingly, the direction of TPW for the last 80 Ma is nearly orthogonal to the great circle about an equatorial axis at 11°E (Figure 6), which is the axis of TPW rotation that would be expected if the Earth's moment of inertia is mainly controlled by the basal mantle structures referred to as large low shear-wave velocity provinces (LLSVPs; Steinberger & Torsvik, 2008; Torsvik et al., 2012, 2014) and that is close to the present-day TPW axis at $\sim 10^\circ\text{E}$ (e.g., Pavoni, 2008). The small component of TPW about this axis for the last 80 Ma is consistent with the findings of Torsvik et al. (2014), who modeled no significant TPW rotations around an equatorial axis located at $0^\circ/11^\circ\text{E}$ for the last 100 Ma (Figure 7a). Instead, our TPWP based on the Müller et al. (2022) frame shows a $\sim 9^\circ$ oscillatory TPW rotation about an axis located at $\sim 85^\circ\text{E}$ (Figures 6 and 7a).

However, the estimated TPW axis between 80 and 120 Ma is closer to the $0^\circ/11^\circ\text{E}$ axis, with an estimated location of the rotation axis based on all four TPWPs at $\sim 34^\circ\text{E}$ (Figure 6a). The TPW axis determined from the three

Figure 2. TPW paths for the last 120 Ma, computed using four different mantle reference frames (a–d). The poles represent the location of the Earth's spin axis relative to a fixed “mean” mantle at 10 Ma steps and are colored by their age. The confidence regions correspond to the paleomagnetic uncertainty only (i.e., the P_{05} of the reference poles of the global APWP, see Vaes et al., 2023). The dashed black line shows the great circle around an equatorial rotation axis at 11°E , corresponding to the preferred TPW axis of Torsvik et al. (2012, 2014). The TPWPs are listed in Table S4 in Supporting Information S1. (e) TPW rate for the last 120 Ma, estimated from each of the four TPW paths. The dashed black line shows the TPW rates derived from the TPW path of Doubrovine et al. (2012).

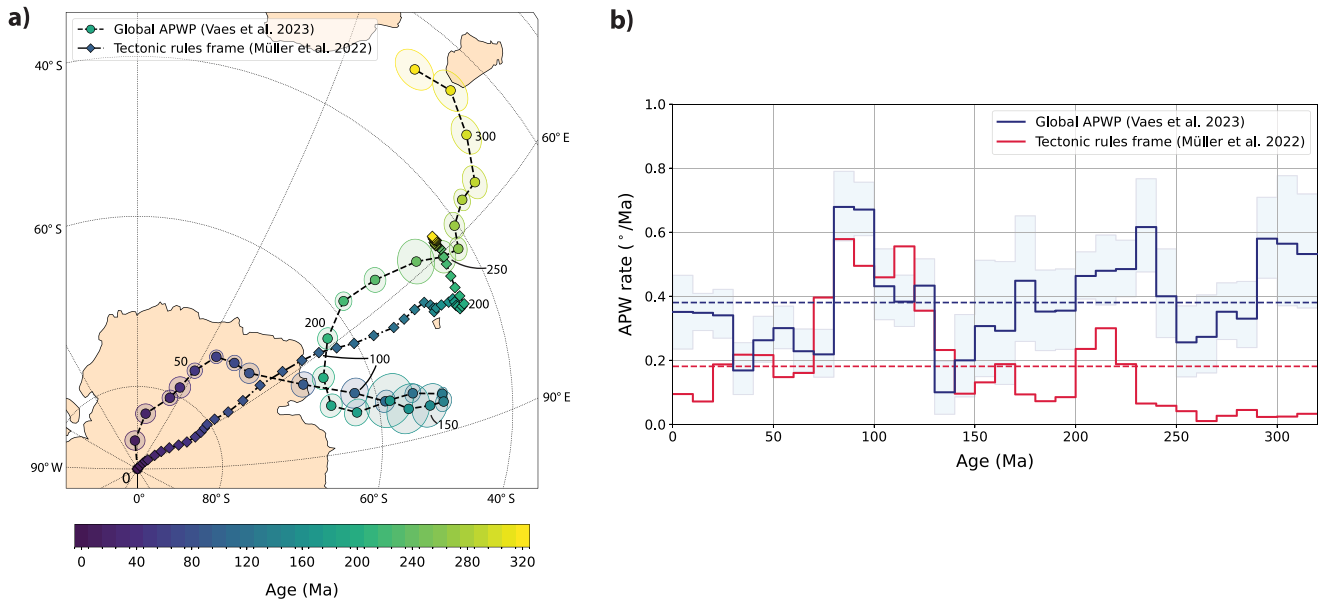


Figure 3. (a) Orthographic plot of the global APWP of Vaes et al. (2023) and the tectonic-rules-based mantle reference frame of Müller et al. (2022). The poles indicate the position of the Earth's spin axis and “mean” mantle relative to a fixed African plate, respectively. (b) Comparison of the apparent polar wander rate derived from the pole paths shows in panel (a). The horizontal dashed lines show the mean rate for the last 320 Ma. The light blue band indicates the 95% confidence limits on the polar wander rate, computed from the uncertainty of the global APWP.

hotspot-based mantle frames is particularly in agreement with this TPW axis, which is also observed from the (sub-)parallel trajectories of the TPWPs to the great-circle about that axis (Figures 2a–2c). The TPWP based on the fixed hotspot frame of Müller et al. (1993) shows the largest rotation of $\sim 15^\circ$ about this axis, between 80 and 120 Ma, although we note that the fixed hotspot model prior to 80 Ma is considered much less reliable (e.g., Torsvik et al., 2008). The previously identified phase of relatively fast TPW ($\sim 0.8^\circ/\text{Ma}$) at 110 and 100 Ma (Steinberger & Torsvik, 2008; Torsvik et al., 2012, 2014) is, however, absent in our TPWPs (Figure 2e). Vaes et al. (2023) showed that a spike in APW between 110 and 100 Ma in the global APWP of Torsvik et al. (2012)

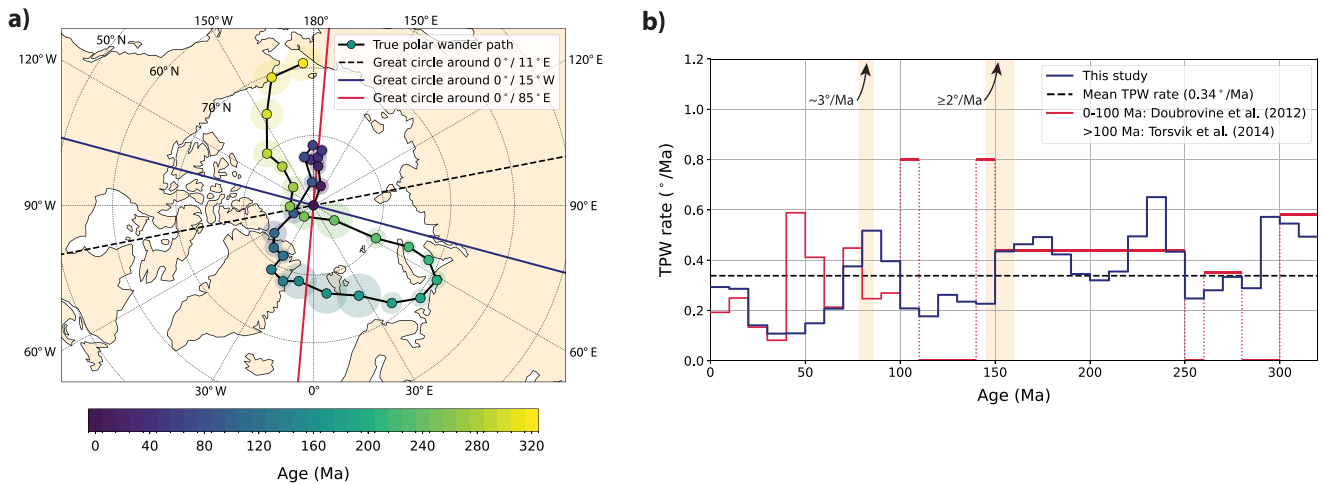


Figure 4. (a) TPW path for the last 320 million years, computed using the tectonic-rules-based reference frame of Müller et al. (2022). Colors and confidence regions are the same as in Figure 2. Great circles around three different TPW axes are shown in blue, red and black (dashed) lines, respectively. (b) The estimated rate of TPW since 320 Ma, computed from the TPW path shown in panel (a). The mean TPW rate ($0.34^\circ/\text{Ma}$) is indicated by the black dashed line. Previously inferred TPW rates by Doubrovine et al. (2012) for the last 100 Ma and by Torsvik et al. (2014) for 100–320 Ma are shown in red. Note that the latter identified distinct “phases” of TPW about a fixed TPW axis at $0^\circ/11^\circ\text{E}$, interspersed by time intervals without significant TPW around this axis. Time intervals for which rapid TPW ($>1^\circ/\text{Ma}$) has been proposed are highlighted by the colored bands: a TPW oscillation with a rate of $\sim 3^\circ/\text{Ma}$ between 86 and 78 Ma (Mitchell et al., 2021) and the Jurassic “monster” polar shift of $\geq 2^\circ/\text{Ma}$ between ~ 160 and 145 Ma (e.g., Kent et al., 2015; Muttoni & Kent, 2019).

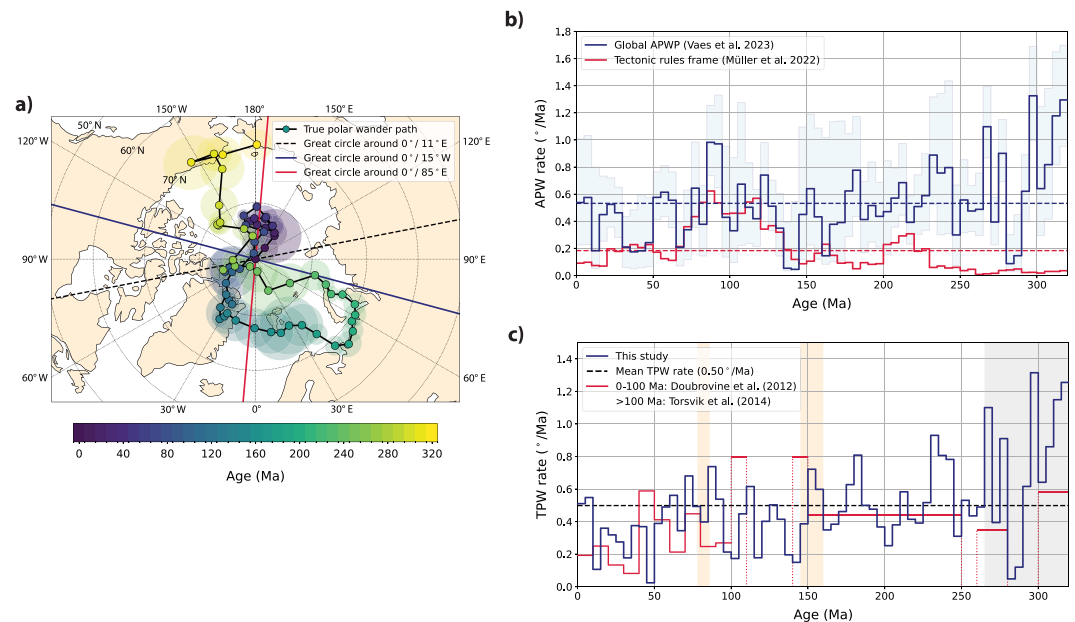


Figure 5. (a) TPW path computed at 5 Ma resolution using the global APWP from Vaes et al. (2023) calculated at a 5 Ma time step using a 10 Ma time window (Table S5 in Supporting Information S1). For more details on the colors, confidence regions and great circles, see Figures 2 and 4. (b) Comparison of the polar wander rates derived from the 5-Ma-resolution global APWP and tectonic-rules-based mantle frame of Müller et al. (2022). The horizontal dashed lines show the mean rates. The light blue band indicates the 95% confidence regions on the rate that is computed from the uncertainty in the 5-Ma-resolution global APWP. (c) Same as Figure 4b, but now showing the TPW rate derived from the 5-Ma-resolution TPW path plotted in panel (a). The gray area highlights the time interval for which the TPW path is less robust, leading to large variations in TPW rate that are likely the result of noise.

was likely the result of temporal bias, and we therefore interpret this inferred 110 and 100 Ma TPW event as a result of this artifact in the underlying APWP.

The TPWP computed for the last 320 Ma shows that TPW predominantly occurred around two equatorial rotation axes that are approximately orthogonal: one axis at $\sim 85^\circ\text{E}$ and a second axis located at $\sim 15^\circ\text{W}$ (Figure 6). Remarkably, the timing and magnitude of TPW along the second axis are very similar to the TPW rotations determined by Torsvik et al. (2012, 2014) based on paleomagnetic data alone (Figure 7), which built upon earlier work by Steinberger and Torsvik (2008). Our new TPWP shows a motion of the spin axis of $\sim 24^\circ$ away from the geographic pole between 260 and 200 Ma, and back parallel to the same great circle and with similar magnitude between 200 and 130 Ma (Figure 7). The inferred rotation axes at a longitude of 15°W is very close to the estimated axes by Steinberger and Torsvik (2008), Torsvik et al. (2012), and Mitchell et al. (2012). These motions would correspond to a coherent counterclockwise rotation of the solid Earth relative to the spin axis between 260 and 200 Ma, followed by a clockwise rotation between 200 and 130 Ma, in agreement with previous findings of, for example, Torsvik et al. (2014). Our results confirm previous inferences by Torsvik et al. (2012, 2014) that cumulative TPW for the last 250 Ma is close to zero (Figure 7b). Finally, we observe a TPW rotation of $\sim 20^\circ$ between 320 and 260 Ma, yielding an angular deviation of the spin axis relative to the mantle of $\sim 20^\circ$ for the Late Carboniferous (~ 320 and 310 Ma). This northward motion of Pangea toward the equator has previously been interpreted as the result of TPW (e.g., Le Pichon et al., 2021). However, in the approach of Torsvik et al. (2012, 2014), Africa is assumed to have remained longitudinally more or less stable and the axis of TPW is fixed at $0^\circ/11^\circ\text{E}$, that is, within Africa. With those underlying assumptions, those studies cannot determine paleolatitudinal motion of Africa (and Pangea) as TPW. The very low absolute plate motion of Africa (and thus Pangea) in the mantle reference frame of Müller et al. (2022) (Figure 3b), which mostly results from minimizing continent motions relative to the mantle, suggests that most of Pangea's paleolatitudinal motion between 320 and 260 Ma is a result of TPW, which has some important implications for the structure of the deep mantle that will be discussed in Section 4.3.

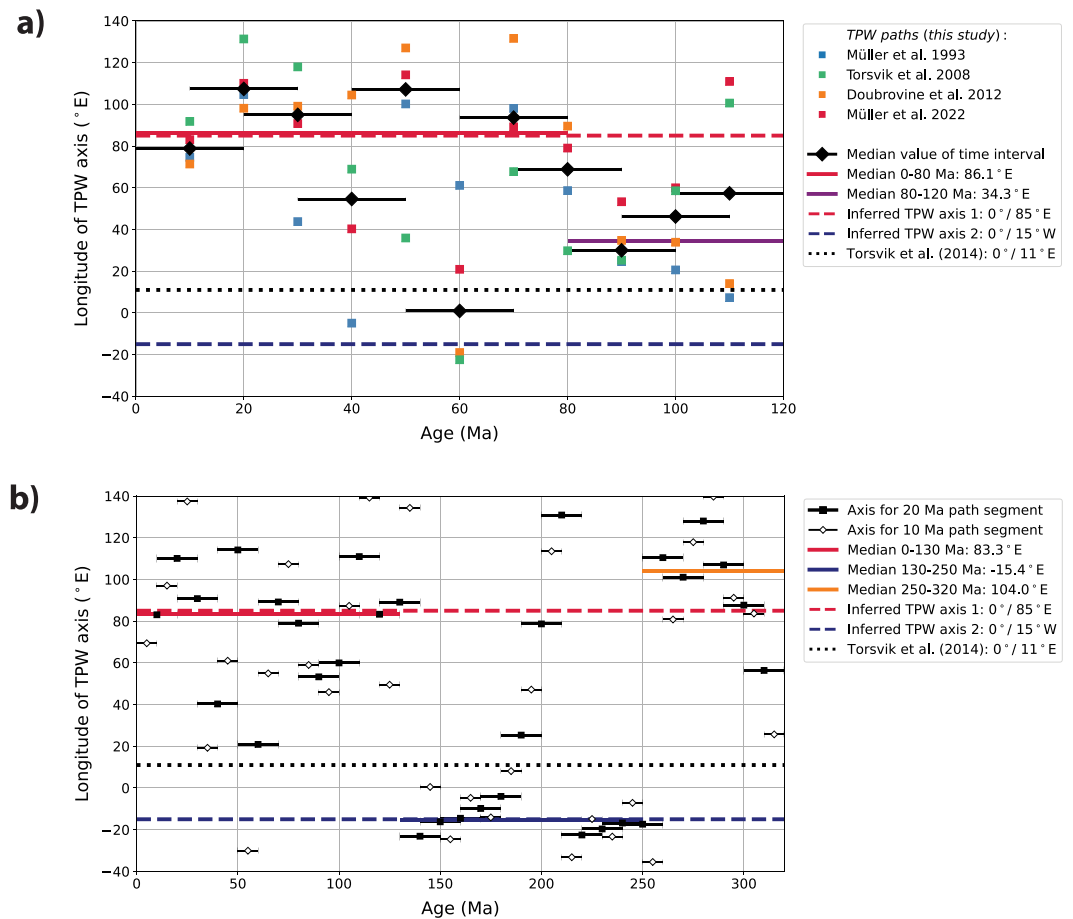


Figure 6. Estimated position of the equatorial axis of TPW. (a) Longitude of the TPW axis computed for 20 Ma segments (e.g., 0–20 Ma, 10–30 Ma) of each TPW path shown in Figures 2a–2d. The median value for each time interval is depicted with the thick black lines and diamonds. The median longitude for the 0–80 Ma and 80–120 Ma time intervals are plotted as red and purple horizontal lines. Inferred main TPW axes are shown as dashed lines. The dotted black line is the preferred axis of TPW from Torsvik et al. (2014). (b) Longitude of the TPW axis determined for both 10 and 20 Ma segments of the TPW path for the last 320 Ma, shown in Figure 4a. Median longitude values are shown for the 0–130, 130–250 and 250–320 Ma intervals.

4.2. True Polar Wander: Not So Fast?

Phases of rapid TPW are frequently proposed based on rapid shifts in paleomagnetic pole positions. The existence of episodic, and possibly oscillatory, phases of rapid TPW are actively investigated by the paleomagnetic community. They are particularly interesting because it may significantly impact regional climate, paleoenvironment, sea level and life (e.g., Jing et al., 2022; Muttoni et al., 2013, 2025; Raub et al., 2007; Wang & Mitchell, 2023). Whether such fast polar shifts truly represent rapid TPW is not always straightforwardly determined, and it may often be difficult to distinguish signal from noise (e.g., Cottrell et al., 2023; Domeier et al., 2023; Evans, 2003; Kulakov et al., 2021). Importantly, the many inherent uncertainties in paleomagnetic data may result in a significant deviation of individual paleomagnetic pole positions from the estimated time-averaged pole given by an APWP, as reflected in the dispersion of poles obtained from similar-aged rocks (Rowley, 2019; Vaes et al., 2022). TPW shifts derived from the data of a single tectonic plate and/or from a small number of paleomagnetic poles, each based on different numbers of paleomagnetic samples/sites and thus averaging the magnetic field to different extents (Vaes et al., 2022), may be prone to unrecognized biases and any conclusions drawn from such analyses should be approached with caution.

For the last 120 Ma, all our TPWPs show a peak in TPW rate during the Late Cretaceous (~80–90 Ma), with a rate of 0.5–0.6°/Ma (Figure 2e). This peak coincides with a phase of fast TPW around 84 Ma that was already

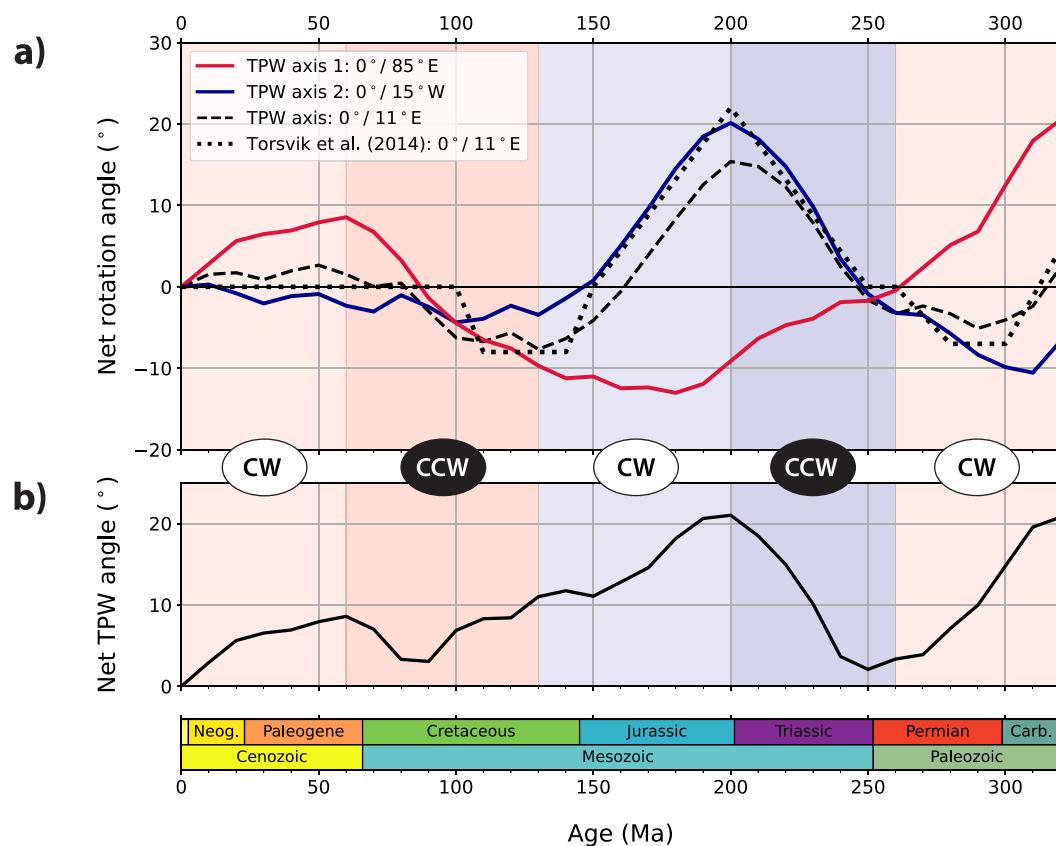


Figure 7. Magnitude of TPW since 320 Ma. (a) Net rotation angle around three different equatorial TPW axes. The angles are computed from the TPW path for the last 320 Ma (Figure 4a) as the total rotation around each axis. Positive values indicate a net clockwise (CW) rotation since that time. Five major, long-term TPW rotations are identified for the last 320 Ma. Clockwise/counterclockwise (CCW) rotations around the inferred TPW axis 1 ($0^{\circ}/85^{\circ}\text{E}$) or TPW axis 2 ($0^{\circ}/15^{\circ}\text{W}$) are shown highlight by light/dark red or blue shading, respectively. The dotted black line shows the estimated net TPW rotations around the preferred TPW axis of $0^{\circ}/11^{\circ}\text{E}$ from Torsvik et al. (2014). (b) Net TPW angle since 320 Ma, computed as the difference between the pole position (i.e., the spin axis) relative to the mantle (i.e., the geographic pole in Figure 4a).

proposed decades ago (e.g., Gordon, 1983; Sager & Koppers, 2000), although these results are not without controversy (e.g., Cottrell & Tarduno, 2000). A recent study by Mitchell et al. (2021) argued for a phase of rapid, oscillatory TPW ($\sim 3^{\circ}/\text{Ma}$) between ~ 86 and 78 Ma, based on high-resolution paleomagnetic records from two partly overlapping stratigraphic sections in northern Italy. Their TPW rates are much higher than obtained in this study (Figures 4b and 5b). However, Cottrell et al. (2023) recently argued that these records contain a secondary overprint overlooked by Mitchell et al. (2021) and interpreted that the section was likely affected by local block rotations, causing a bias in the paleomagnetic directions and casting doubt on this interpreted fast TPW event.

The most notable potential episode of rapid TPW is the Jurassic “monster” polar shift: a ~ 30 – 40° shift in pole position in the APWP of North America between ~ 160 and 145 Ma (Kent et al., 2015; Muttoni & Kent, 2019). Paleomagnetic data obtained from Upper Jurassic carbonates of the continental block of Adria, under the assumption that Adria was rigidly attached to Africa since the opening of the Ionian Sea between 170 and 154 Ma (Channell et al., 2022), also show a $\sim 30^{\circ}$ shift in pole position in North American coordinates (Muttoni & Kent, 2019; Muttoni et al., 2025). However, the reliability of key paleomagnetic poles from North American kimberlites as well as the assumption that Adria was rigidly attached to northern Africa have been challenged (e.g., Kulakov et al., 2021; Mirzaei et al., 2021; van Hinsbergen et al., 2020). The differences in Late Jurassic APWPs and associated estimates of TPW mostly result from differences in data selection, reflecting contrasting views on which paleomagnetic poles can be reliably used in paleomagnetic analyses (Kulakov et al., 2021; Mirzaei et al., 2025; Muttoni et al., 2025; Muttoni & Kent, 2019). Since TPW affects all tectonic plates and continents

simultaneously, the existence of a rapid TPW phase may be tested at different (paleo-)locations. Intriguingly, different paleomagnetic data sets from a range of tectonic plates provide both evidence in support of fast polar motion during the Late Jurassic, such as from North China (Yi et al., 2019), the Lhasa terrane (Ma et al., 2022) and the Pacific plate (Fu & Kent, 2018), or against it, such as from North China (Gao et al., 2021), Greenland (Kulakov et al., 2021) and South America (Ruiz González et al., 2022).

Our results, based on a global APWP in which temporal and spatial uncertainties in the underlying paleomagnetic data are incorporated, do not provide any clear evidence for phases of rapid ($>1.0^\circ/\text{Ma}$) TPW of >10 Ma during the last 320 Ma (Figures 4b and 5c). We acknowledge that the absence of relatively fast TPW maybe a consequence of using a 20 Ma time window for the global APWP that underlies the TPWPs presented here. This may smoothen or obscure potential short-term (<10 Ma) and/or small-amplitude phases of rapid polar wander (e.g., Mitchell et al., 2021; Muttoni et al., 2005, 2025). It is interesting to note, however, that the highest TPW rates are observed during the middle of a long, large-amplitude TPW rotation (Figure 4b). This is consistent with theoretical inferences that the fastest TPW is expected to occur during longer term episodes of TPW (Cottrell et al., 2023; Goldreich & Toomre, 1969; Tsai & Stevenson, 2007). We indeed observe that TPW rate accelerates until a peak velocity is reached before decelerating again, such that the fastest TPW rate during each long-term TPW rotation (see Figure 7) is greater than the average TPW rate for that rotation (Figure 4b). Then again, even when computing a TPWP at 5 Ma resolution and with a 10 Ma time window, we do not find clear evidence for TPW occurring at velocities beyond $1^\circ/\text{Ma}$. The peaks in TPW rate of more than $1.0^\circ/\text{Ma}$ observed for the 5-Ma-resolution TPWP (Figure 5c) are not statistically significant and do not follow the expected velocity pattern clearly observed for the 10-Ma-resolution TPWP, and we therefore conservatively interpret these as noise rather than a true “signal.”

To establish whether phases of fast ($>1^\circ/\text{Ma}$) TPW of <10 Ma have occurred since the Late Paleozoic requires an increase in the resolution of the APWPs used to quantify TPW, as well as the quantification of the uncertainty in the mantle reference frame. Before these become available, such rapid changes in pole position may instead be identified by collecting well-dated, paleomagnetic data sets from sedimentary sequences with a high sampling resolution, which may provide high-resolution records of shifts in the paleomagnetic declination and inclination (e.g., Mitchell et al., 2021; Vaes et al., 2021). However, observed shifts in the paleomagnetic direction may result from paleomagnetic and/or tectonic artifacts, and should be thoroughly tested for potential biases. The collection of multiple high-resolution paleomagnetic records from stratigraphic sections of overlapping age and from different tectonic plates provides a way to test whether an observed rapid polar shift may indeed represent TPW. In addition, higher-resolution APWPs computed from site-level paleomagnetic data using a bottom-up uncertainty propagation scheme (Gallo et al., 2023) may allow the identification of fast and short-lived phases of TPW.

4.3. Linking True Polar Wander and Mantle Dynamics

The rate of TPW provides first-order kinematic constraints on the rate of mantle convection, particularly on the velocity at which density anomalies, such as sinking lithospheric slabs, move through the Earth's mantle. Fu et al. (2022) presented a compilation of paleomagnetically estimated TPW rates since the late Mesoproterozoic ($\sim 1,100$ Ma), proposing a direct link between the secular change of the TPW rate and the thermal structure and nature of convection in the mantle. Fast TPW ($>1^\circ/\text{Ma}$) has often been inferred for pre-Pangean TPW, suggesting a different geodynamic regime that may correlate with the supercontinent cycle (e.g., Evans, 2003; Fu et al., 2022; Mitchell, 2014). Testing pre-Mesozoic TPW hypotheses is not straightforward, as plate motion-induced polar wander may be difficult to distinguish from TPW and thus obscure past TPW signals (Evans, 2003; Torsvik et al., 2014). Moreover, rapid polar shifts of up to $\sim 90^\circ$ during the Early Cambrian and Ediacaran have also been attributed to TPW (e.g., Kirschvink et al., 1997; Mitchell et al., 2011; Robert et al., 2017), but may alternatively be explained by unusual geomagnetic field behavior (Domeier et al., 2023; Robert et al., 2023).

Reproducing observed TPW by numerical modeling has also proven difficult, as this requires detailed knowledge on the structure of the mantle, such as the volumes and distribution of subducted lithospheric slabs (see Steinberger & Torsvik, 2010). Paleomagnetism-based estimates of TPW rates are frequently compared to TPW speed limits inferred from geodynamic modeling. However, these predictions vary substantially. For instance, Tsai and Stevenson (2007) provide a theoretical speed limit of $2.4^\circ/\text{Ma}$ but find a maximum TPW shift of 8° for a period of 10 Ma (corresponding to $0.8^\circ/\text{Ma}$). On the other hand, Greff-Lefftz and Besse (2014) argue that TPW may occur at rates of up to $10^\circ/\text{Ma}$ for larger mass reorganizations. These estimates heavily rely on the choice of rheological

parameters, which are poorly constrained, particularly for deep geological time (Steinberger & Torsvik, 2010; Tsai & Stevenson, 2007). Moreover, such geodynamic models used to determine the magnitude and rate of TPW tend to have slab sinking rates that are higher than independent kinematic constraints on the slab sinking velocity versus depth, such as those obtained from seismic tomographic images of subducted slabs (e.g., van der Meer et al., 2018; van der Wiel et al., 2024). The TPW rates predicted by those models are thus likely upper estimates.

Recent modeling studies show that TPW rotations are likely stabilized by the contribution to the moment of inertia by the two antipodal LLSVPs, with important contributions from subducted slabs, whose relative contribution to the moment of inertia strongly change with depth (e.g., Greff-Lefftz & Besse, 2012; Steinberger et al., 2017; Steinberger & Torsvik, 2010). Observed TPW rotations about an axis of minimum moment of inertia that is close to the combined center of mass of the LLSVPs suggests that TPW may be controlled by these structures (Torsvik et al., 2012, 2014). TPW rotations along an axis nearly orthogonal to this $0^{\circ}/11^{\circ}\text{E}$ axis (see Figures 6 and 7) instead indicate that the reorientation of the solid Earth may (also) be controlled by other contributions to the moment of inertia tensor, for example, resulting from large density anomalies caused by subducting slabs at relatively high latitudes $\sim 90^{\circ}$ from this alternative axis (Steinberger & Torsvik, 2010). If driven by changes in subduction configuration and slab sinking, the two approximately orthogonal axes of TPW identified here (Figures 6 and 7) roughly coincide with low-latitude subduction in the Tethyan realm for the $\sim 0^{\circ}/15^{\circ}\text{E}$ axis, whereas the $\sim 0^{\circ}/85^{\circ}\text{E}$ axis would correspond to changes in subduction flux in the Pacific realm. Our calculations show that the magnitudes of TPW are roughly equal for the two, or even slightly larger for the effects of Tethyan subduction, even though Tethyan subduction occurs at much lower latitudes than Pacific subduction (e.g., Boschman et al., 2021; Seton et al., 2012; Vaes et al., 2019). This may illustrate the stabilizing effects of LLSVPs and could allow the detailed computation of their absolute density from their contribution to the moment of inertia.

Intriguingly, our results show a $\sim 20^{\circ}$ TPW rotation for the time interval between 320 and 260 Ma around an axis orthogonal to $0^{\circ}/11^{\circ}\text{E}$ axis (Figure 7a). This would identify the well-constrained northward motion of Pangea during this time interval as largely a result of TPW (Le Pichon et al., 2021; Marcano et al., 1999). This is surprising, given that the LLSVPs are thought to dominate the present-day moment of inertia of the Earth (Steinberger & Torsvik, 2010) and may have remained stable and antipodal throughout the entire Phanerozoic (Torsvik et al., 2014). If correct, this TPW rotation would imply that the contribution of other density anomalies than the LLSVPs, likely high-latitude slabs, may contribute sufficiently to the total moment of inertia to allow them to rotate $\sim 20^{\circ}$ relative to the spin axis toward the equatorial plane. This could be explained by either a different mantle viscosity and/or density structure during the (Late) Paleozoic, for example, driven by a large volume of subducting slabs surrounding Pangea that drove the supercontinent and its surrounding subduction zones toward the equator. Alternatively, this may be explained by LLSVPs that were smaller, less dense, or mobile prior to ~ 260 Ma. We note, however, that the estimates of pre-260 Ma TPW are strongly influenced by the choices in either reference frame computation (the “tectonic-rules-based” mantle reference frame of Müller et al. (2022) that keeps Pangea nearly fixed to the ambient mantle to reduce continental plate motion) or TPW computation (keeping the TPW axis fixed at $0^{\circ}/11^{\circ}\text{E}$, Torsvik et al., 2014).

Finally, the computation of TPW requires knowledge of absolute plate motion in the paleomagnetic and mantle reference frames. The former requires that the time-averaged geomagnetic field aligns with the Earth's spin axis and that paleomagnetic data provide an accurate approximation of the mean pole position. Recent analysis has shown that even higher-resolution and more precise APWPs may be computed when uncertainty is propagated from site-level paleomagnetic data using a bottom-up approach (Gallo et al., 2023). Moreover, we emphasize that to establish whether observed TPW is statistically significant, and to assess the robustness of TPW rates and its implications for mantle dynamics, it is key to improve the quantification of uncertainties in mantle reference frames, such as the incorporation of uncertainties in absolute plate rotations (e.g., Doubrovine et al., 2012). Defining a robust mantle reference frame with uncertainty quantification remains a key challenge for solid Earth science. All our attempts to define a mantle reference frame will inevitably remain approximations, since we are treating a convecting mantle as a fixed frame of reference. However, in a mantle frame based on simple “tectonic rules,” TPW becomes an intrinsic property of the mantle reference frame. This way, numerical models of global mantle convection driven by plate tectonics in an assumed mantle reference frame may then be calibrated against TPW, and iterated, along with hotspot tracks in an iterative modeling approach as in, for example, Doubrovine et al. (2012). This may not only provide novel constraints on mantle dynamics research but also allow the identification of the dynamic drivers of TPW. Lastly, we foresee that improved observational constraints on the

timing, rate, and magnitude of TPW will contribute to exploring the exciting links between TPW and Earth's climate, hydrosphere, cryosphere, geodynamo, and biosphere in the geological past.

5. Conclusions

Here, we present new quantitative estimates of TPW since 320 Ma. We find that TPW since 320 Ma occurred as large ($>10^\circ$) but slow rotations at rates typically below $0.5^\circ/\text{Ma}$, with a mean TPW rate of $0.34^\circ \pm 0.14^\circ/\text{Ma}$ (1σ). The TPW paths computed using four different mantle reference frames all show significant ($>5^\circ$) TPW since 100 Ma, in contrast to some recent studies. The TPW path back to 320 Ma supports the existence of multiple large TPW oscillations of up to $\sim 20^\circ$ since the Permian. We find no evidence for phases of fast ($>1^\circ/\text{Ma}$) TPW on timescales of >10 Ma, suggesting that previously observed, and heavily debated, rapid TPW may be an artifact. Our results show that TPW since 320 Ma predominantly occurred around two nearly orthogonal equatorial axes. We confirm a previously constrained oscillatory TPW rotation of $\sim 24^\circ$ in the Triassic and Jurassic around an axis that is close to the present-day center of mass of the antipodal LLSVPs in the lowermost mantle. In contrast, TPW is shown to have occurred about an axis at $\sim 85^\circ\text{E}$ during the last ~ 80 Ma and between 260 and 320 Ma, implying that other contributions to the moment of inertia, such as those exerted by subducting lithospheric slabs, controlled the nature of TPW. We tentatively explain the changes in the dominant axis of TPW since 320 Ma to changes in the contribution to the moment of inertia of low-latitude Tethyan subduction versus higher-latitude subduction in the Pacific realm. The $>20^\circ$ TPW oscillation around an axis close to the center of LLSVPs may confirm the stabilizing effects of LLSVPs on Earth's moment of inertia. Finally, we highlight that the coupling of kinematic constraints on TPW with absolute plate motion models provides an opportunity for calibration of numerical experiments of mantle dynamics.

Conflict of Interest

The authors declare no conflicts of interest relevant to this study.

Data Availability Statement

The Jupyter Notebook and input files used for the analyses in this study are publicly available on GitHub (<https://github.com/bramvaes/TPW>) and are archived on Zenodo (Vaes, 2025). We acknowledge the use of the freely available paleomagnetic software package PmagPy (Tauxe et al., 2016) in the Python codes used to perform the calculations. The complete paleomagnetic database that underpins the global APWP of Vaes et al. (2023) is available as Supplementary Datafile to the online version of that publication, as well as on the Reference database portal on [APWP-online.org](https://www.apwp-online.org) (Vaes et al., 2024).

Acknowledgments

This study was supported by the Netherlands Organization for Scientific Research (NWO Vici Grant 865.17.001 to DJJvH). We thank Richard Gordon, Jean Besse, and two anonymous reviewers for their constructive feedback and helpful suggestions. We also thank Bernhard Steinberger, Jonny Wu, Chris Calvelage, and Dennis Kent for discussion. Open access publishing facilitated by Università degli Studi di Milano-Bicocca, as part of the Wiley - CRUI-CARE agreement.

References

- Andrews, J. A. (1985). True polar wander: An analysis of Cenozoic and Mesozoic paleomagnetic poles. *Journal of Geophysical Research*, *90*(B9), 7737–7750. <https://doi.org/10.1029/jb090ib09p07737>
- Besse, J., & Courtillot, V. (2002). Apparent and true polar wander and the geometry of the geomagnetic field over the last 200 Myr. *Journal of Geophysical Research*, *107*(B11), EPM-6. <https://doi.org/10.1029/2000jb000050>
- Besse, J., Courtillot, V., & Greff, M. (2021). Paleomagnetism, polar wander. In H. K. Gupta (Ed.), *Encyclopedia of solid Earth geophysics. Encyclopedia of Earth sciences series*. Springer.
- Biggin, A. J., Steinberger, B., Aubert, J., Suttie, N., Holme, R., Torsvik, T. H., et al. (2012). Possible links between long-term geomagnetic variations and whole-mantle convection processes. *Nature Geoscience*, *5*(8), 526–533. <https://doi.org/10.1038/ngeo1521>
- Boschman, L. M., Van Hinsbergen, D. J., Langereis, C. G., Flores, K. E., Kamp, P. J., Kimbrough, D. L., et al. (2021). Reconstructing lost plates of the Panthalassa Ocean through paleomagnetic data from circum-Pacific accretionary orogens. *American Journal of Science*, *321*(6), 907–954. <https://doi.org/10.2475/06.2021.08>
- Channell, J. E., Muttoni, G., & Kent, D. V. (2022). Adria in mediterranean paleogeography, the origin of the Ionian Sea, and Permo-Triassic configurations of Pangea. *Earth-Science Reviews*, *230*, 104045. <https://doi.org/10.1016/j.earscirev.2022.104045>
- Cottrell, R. D., Bono, R. K., Channell, J. E., Bunge, H. P., & Tarduno, J. A. (2023). No Late Cretaceous true polar wander oscillation and implications for stability of Earth relative to the rotation axis. *Earth and Planetary Science Letters*, *620*, 118338. <https://doi.org/10.1016/j.epsl.2023.118338>
- Cottrell, R. D., & Tarduno, J. A. (2000). Late Cretaceous true polar wander: Not so fast. *Science*, *288*(5475), 2283. <https://doi.org/10.1126/science.288.5475.2283a>
- Domeier, M., Robert, B., Meert, J. G., Kulakov, E. V., McCausland, P. J., Trindade, R. I., & Torsvik, T. H. (2023). The enduring Ediacaran paleomagnetic enigma. *Earth-Science Reviews*, *242*, 104444. <https://doi.org/10.1016/j.earscirev.2023.104444>
- Dobrovine, P. V., Steinberger, B., & Torsvik, T. H. (2012). Absolute plate motions in a reference frame defined by moving hot spots in the Pacific, Atlantic, and Indian Oceans. *Journal of Geophysical Research*, *117*(B9). <https://doi.org/10.1029/2011jb009072>
- Evans, D. A. (2003). True polar wander and supercontinents. *Tectonophysics*, *362*(1–4), 303–320. [https://doi.org/10.1016/s0040-1951\(02\)000642-x](https://doi.org/10.1016/s0040-1951(02)000642-x)

- Fu, H., Zhang, S., Condon, D. J., & Xian, H. (2022). Secular change of true polar wander over the past billion years. *Science Advances*, 8(41), eabo2753. <https://doi.org/10.1126/sciadv.abo2753>
- Fu, R. R., & Kent, D. V. (2018). Anomalous Late Jurassic motion of the Pacific Plate with implications for true polar wander. *Earth and Planetary Science Letters*, 490, 20–30. <https://doi.org/10.1016/j.epsl.2018.02.034>
- Gallo, L. C., Domeier, M., Sapienza, F., Swanson-Hysell, N. L., Vaes, B., Zhang, Y., et al. (2023). Embracing uncertainty to resolve polar wander: A case study of Cenozoic North America. *Geophysical Research Letters*, 50(11), e2023GL103436. <https://doi.org/10.1029/2023gl103436>
- Gao, Y., Zhang, S., Zhao, H., Ren, Q., Yang, T., Wu, H., & Li, H. (2021). North China block underwent simultaneous true polar wander and tectonic convergence in late Jurassic: New paleomagnetic constraints. *Earth and Planetary Science Letters*, 567, 117012. <https://doi.org/10.1016/j.epsl.2021.117012>
- Gold, T. (1955). Instability of the Earth's axis of rotation. *Nature*, 175(4456), 526–529. <https://doi.org/10.1038/175526a0>
- Goldreich, P., & Toomre, A. (1969). Some remarks on polar wandering. *Journal of Geophysical Research*, 74(10), 2555–2567. <https://doi.org/10.1029/jb074i010p02555>
- Gordon, R. G. (1983). Late Cretaceous apparent polar wander of the Pacific plate: Evidence for a rapid shift of the Pacific hotspots with respect to the spin axis. *Geophysical Research Letters*, 10(8), 709–712. <https://doi.org/10.1029/gl10i008p00709>
- Gradstein, F. M., Ogg, J. G., Schmitz, M. D., & Ogg, G. M. (2020). *Geologic time scale 2020*. Elsevier.
- Greff-Lefftz, M., & Besse, J. (2012). Paleomovement of continents since 300 Ma, mantle dynamics and large wander of the rotational pole. *Earth and Planetary Science Letters*, 345, 151–158. <https://doi.org/10.1016/j.epsl.2012.06.017>
- Greff-Lefftz, M., & Besse, J. (2014). Sensitivity experiments on True Polar Wander. *Geochemistry, Geophysics, Geosystems*, 15(12), 4599–4616. <https://doi.org/10.1002/2014GC005504>
- Jing, X., Yang, Z., Mitchell, R. N., Tong, Y., Zhu, M., & Wan, B. (2022). Ordovician–Silurian true polar wander as a mechanism for severe glaciation and mass extinction. *Nature Communications*, 13(1), 7941. <https://doi.org/10.1038/s41467-022-35609-3>
- Jurdy, D. M., & Van der Voo, R. (1974). A method for the separation of true polar wander and continental drift, including results for the last 55 my. *Journal of Geophysical Research*, 79(20), 2945–2952. <https://doi.org/10.1029/jb079i020p02945>
- Kent, D. V., & Irving, E. (2010). Influence of inclination error in sedimentary rocks on the Triassic and Jurassic apparent pole wander path for North America and implications for Cordilleran tectonics. *Journal of Geophysical Research*, 115(B10). <https://doi.org/10.1029/2009jb007205>
- Kent, D. V., Kjarsgaard, B. A., Gee, J. S., Muttoni, G., & Heaman, L. M. (2015). Tracking the Late Jurassic apparent (or true) polar shift in U-Pb-dated kimberlites from cratonic North America (Superior Province of Canada). *Geochemistry, Geophysics, Geosystems*, 16(4), 983–994. <https://doi.org/10.1002/2015gc005734>
- Kirschvink, J. L., Ripperdan, R. L., & Evans, D. A. (1997). Evidence for a large-scale reorganization of Early Cambrian continental masses by inertial interchange true polar wander. *Science*, 277(5325), 541–545. <https://doi.org/10.1126/science.277.5325.541>
- Kulakov, E. V., Torsvik, T. H., Doubrovine, P. V., Slagstad, T., Ganerød, M., Silkoset, P., & Werner, S. C. (2021). Jurassic fast polar shift rejected by a new high-quality paleomagnetic pole from southwest Greenland. *Gondwana Research*, 97, 240–262. <https://doi.org/10.1016/j.gr.2021.05.021>
- Le Pichon, X., Jellinek, M., Lenardic, A., Şengör, A. C., & İmren, C. (2021). Pangea migration. *Tectonics*, 40(6), e2020TC006585. <https://doi.org/10.1029/2020tc006585>
- Livermore, R. A., Vine, F. J., & Smith, A. G. (1984). Plate motions and the geomagnetic field—II. Jurassic to Tertiary. *Geophysical Journal International*, 79(3), 939–961. <https://doi.org/10.1111/j.1365-246x.1984.tb02878.x>
- Ma, Y., Wang, Q., Wang, H., Wan, B., Zhang, S., Deng, C., et al. (2022). Jurassic paleomagnetism of the Lhasa terrane—Implications for Tethys evolution and true polar wander. *Journal of Geophysical Research: Solid Earth*, 127(12), e2022JB025577. <https://doi.org/10.1029/2022jb025577>
- Marcano, M. C., Van der Voo, R., & Mac Niocaill, C. (1999). True polar wander during the Permo-Triassic. *Journal of Geodynamics*, 28(2–3), 75–95. [https://doi.org/10.1016/s0264-3707\(98\)00026-x](https://doi.org/10.1016/s0264-3707(98)00026-x)
- Merdith, A. S., Williams, S. E., Collins, A. S., Tetley, M. G., Mulder, J. A., Blades, M. L., et al. (2021). Extending full-plate tectonic models into deep time: Linking the Neoproterozoic and the Phanerozoic. *Earth-Science Reviews*, 214, 103477. <https://doi.org/10.1016/j.earscirev.2020.103477>
- Mirzaei, M., Burmester, R. F., Housen, B. A., & Kravchinsky, V. A. (2025). Paleomagnetic consequence of thermal evolution of the North American passive margin: The Jurassic APWP controversy. *Gondwana Research*, 140, 89–100. <https://doi.org/10.1016/j.gr.2025.01.007>
- Mirzaei, M., Housen, B. A., Burmester, R. F., & Foreman, B. Z. (2021). Paleomagnetic results from Upper Triassic and Middle Jurassic strata of east-central New Mexico, and implication for North American apparent polar wander path. *Tectonophysics*, 811, 228872. <https://doi.org/10.1016/j.tecto.2021.228872>
- Mitchell, R. N. (2014). True polar wander and supercontinent cycles: Implications for lithospheric elasticity and the triaxial Earth. *American Journal of Science*, 314(5), 966–979. <https://doi.org/10.2475/05.2014.04>
- Mitchell, R. N., Kilian, T. M., & Evans, D. A. (2012). Supercontinent cycles and the calculation of absolute palaeolongitude in deep time. *Nature*, 482(7384), 208–211. <https://doi.org/10.1038/nature10800>
- Mitchell, R. N., Kilian, T. M., Raub, T. D., Evans, D. A., Bleeker, W., & Maloof, A. C. (2011). Sutton hotspot: Resolving Ediacaran-Cambrian tectonics and true polar wander for Laurentia. *American Journal of Science*, 311(8), 651–663. <https://doi.org/10.2475/08.2011.01>
- Mitchell, R. N., Thissen, C. J., Evans, D. A., Slotznick, S. P., Coccioni, R., Yamazaki, T., & Kirschvink, J. L. (2021). A Late Cretaceous true polar wander oscillation. *Nature Communications*, 12(1), 3629. <https://doi.org/10.1038/s41467-021-23803-8>
- Morgan, W. J. (1971). Convection plumes in the lower mantle. *Nature*, 230(5288), 42–43. <https://doi.org/10.1038/230042a0>
- Morgan, W. J. (1981). Hotspot tracks and the opening of the Atlantic and Indian Oceans. *The Oceanic Lithosphere*, 7, 443–487.
- Müller, R. D., Flament, N., Cannon, J., Tetley, M. G., Williams, S. E., Cao, X., et al. (2022). A tectonic-rules-based mantle reference frame since 1 billion years ago—implications for supercontinent cycles and plate–mantle system evolution. *Solid Earth*, 13(7), 1127–1159. <https://doi.org/10.5194/se-13-1127-2022>
- Muttoni, G., Dallanave, E., & Channell, J. E. T. (2013). The drift history of Adria and Africa from 280 Ma to Present, Jurassic true polar wander, and zonal climate control on Tethyan sedimentary facies. *Palaeogeography, Palaeoclimatology, Palaeoecology*, 386, 415–435. <https://doi.org/10.1016/j.palaeo.2013.06.011>
- Muttoni, G., Dallanave, E., & Della, P. G. (2025). European arid anomaly explained with southward drift of Eurasia during the late Jurassic polar shift. *Geochemistry, Geophysics, Geosystems*, 26(2), e2024GC011730. <https://doi.org/10.1029/2024gc011730>
- Muttoni, G., Erba, E., Kent, D. V., & Bachtadse, V. (2005). Mesozoic Alpine facies deposition as a result of past latitudinal plate motion. *Nature*, 434(7029), 59–63. <https://doi.org/10.1038/nature03378>
- Muttoni, G., & Kent, D. V. (2019). Jurassic monster polar shift confirmed by sequential paleopoles from Adria, promontory of Africa. *Journal of Geophysical Research: Solid Earth*, 124(4), 3288–3306. <https://doi.org/10.1029/2018jb017199>

- Müller, R. D., Royer, J. Y., & Lawver, L. A. (1993). Revised plate motions relative to the hotspots from combined Atlantic and Indian Ocean hotspot tracks. *Geology*, *21*(3), 275–278. [https://doi.org/10.1130/0091-7613\(1993\)021<0275:rpmrt>2.3.co;2](https://doi.org/10.1130/0091-7613(1993)021<0275:rpmrt>2.3.co;2)
- O'Neill, C., Müller, D., & Steinberger, B. (2005). On the uncertainties in hot spot reconstructions and the significance of moving hot spot reference frames. *Geochemistry, Geophysics, Geosystems*, *6*(4). <https://doi.org/10.1029/2004gc000784>
- Pavoni, N. (2008). Present true polar wander in the frame of the Geotectonic Reference System. *Swiss Journal of Geosciences*, *101*(3), 629–636. <https://doi.org/10.1007/s00015-008-1284-y>
- Raub, T. D., Kirschvink, J. L., & Evans, D. A. D. (2007). True polar wander: Linking deep and shallow geodynamics to hydro- and bio-spheric hypotheses. *Treatise on geophysics*, *5*, 565–589. <https://doi.org/10.1016/b978-0-444-52748-6.00099-7>
- Robert, B., Besse, J., Blein, O., Greff-Lefftz, M., Baudin, T., Lopes, F., et al. (2017). Constraints on the Ediacaran inertial interchange true polar wander hypothesis: A new paleomagnetic study in Morocco (west African Craton). *Precambrian Research*, *295*, 90–116. <https://doi.org/10.1016/j.precamres.2017.04.010>
- Robert, B., Corfu, F., Domeier, M., & Blein, O. (2023). Evidence for large disturbances of the Ediacaran geomagnetic field from West Africa. *Precambrian Research*, *394*, 107095. <https://doi.org/10.1016/j.precamres.2023.107095>
- Rose, L., & Buffett, B. (2017). Scaling rates of true polar wander in convecting planets and moons. *Physics of the Earth and Planetary Interiors*, *273*, 1–10. <https://doi.org/10.1016/j.pepi.2017.10.003>
- Rowley, D. B. (2019). Comparing paleomagnetic study means with apparent wander paths: A case study and paleomagnetic test of the greater India versus greater Indian basin hypotheses. *Tectonics*, *38*(2), 722–740. <https://doi.org/10.1029/2017tc004802>
- Ruiz González, V., Renda, E. M., Vizán, H., Ganerød, M., Puigdomenech, C. G., & Zaffarana, C. B. (2022). Deformation along the Deseado Massif (Patagonia, Argentina) during the Jurassic period and its relationship with the Gondwana breakup: Paleomagnetic and geochronological constraints. *Tectonophysics*, *834*, 229389. <https://doi.org/10.1016/j.tecto.2022.229389>
- Sager, W. W., & Koppers, A. A. A. (2000). Late Cretaceous polar wander of the Pacific plate: Evidence of a rapid true polar wander event. *Science*, *287*(5452), 455–459. <https://doi.org/10.1126/science.287.5452.455>
- Seton, M., Müller, R. D., Zahirovic, S., Gaina, C., Torsvik, T., Shephard, G., et al. (2012). Global continental and ocean basin reconstructions since 200 Ma. *Earth-Science Reviews*, *113*(3–4), 212–270. <https://doi.org/10.1016/j.earscirev.2012.03.002>
- Spada, G., Ricard, Y., & Sabadini, R. (1992). Excitation of true polar wander by subduction. *Nature*, *360*(6403), 452–454. <https://doi.org/10.1038/360452a0>
- Steinberger, B., Seidel, M. L., & Torsvik, T. H. (2017). Limited true polar wander as evidence that Earth's nonhydrostatic shape is persistently triaxial. *Geophysical Research Letters*, *44*(2), 827–834. <https://doi.org/10.1002/2016gl071937>
- Steinberger, B., & Torsvik, T. H. (2008). Absolute plate motions and true polar wander in the absence of hotspot tracks. *Nature*, *452*(7187), 620–623. <https://doi.org/10.1038/nature06824>
- Steinberger, B., & Torsvik, T. H. (2010). Toward an explanation for the present and past locations of the poles. *Geochemistry, Geophysics, Geosystems*, *11*(6). <https://doi.org/10.1029/2009gc002889>
- Tauxe, L., Shaar, R., Jonestrask, L., Swanson-Hysell, N. L., Minnett, R., Koppers, A. A. P., et al. (2016). PmagPy: Software package for paleomagnetic data analysis and a bridge to the magnetism information consortium (MagIC) database. *Geochemistry, Geophysics, Geosystems*, *17*(6), 2450–2463. <https://doi.org/10.1002/2016gc006307>
- Tetley, M. G., Williams, S. E., Gurnis, M., Flament, N., & Müller, R. D. (2019). Constraining absolute plate motions since the Triassic. *Journal of Geophysical Research: Solid Earth*, *124*(7), 7231–7258. <https://doi.org/10.1029/2019jb017442>
- Torsvik, T. H., Müller, R. D., Van der Voo, R., Steinberger, B., & Gaina, C. (2008). Global plate motion frames: Toward a unified model. *Reviews of Geophysics*, *46*(3). <https://doi.org/10.1029/2007rg000227>
- Torsvik, T. H., van der Voo, R., Doubrovine, P. V., Burke, K., Steinberger, B., Ashwal, L. D., et al. (2014). Deep mantle structure as a reference frame for movements in and on the Earth. *Proceedings of the National Academy of Sciences*, *111*(24), 8735–8740. <https://doi.org/10.1073/pnas.1318135111>
- Torsvik, T. H., van der Voo, R., Preeden, U., Mac Niocaill, C., Steinberger, B., Doubrovine, P. V., et al. (2012). Phanerozoic polar wander, palaeogeography and dynamics. *Earth-Science Reviews*, *114*(3–4), 325–368. <https://doi.org/10.1016/j.earscirev.2012.06.007>
- Tsai, V. C., & Stevenson, D. J. (2007). Theoretical constraints on true polar wander. *Journal of Geophysical Research*, *112*(B5). <https://doi.org/10.1029/2005jb003923>
- Vaes, B. (2025). Software for: “Slow true polar wander around varying equatorial axes since 320 Ma” [Software]. *Zenodo*. <https://doi.org/10.5281/zenodo.14944326>
- Vaes, B., Gallo, L. C., & van Hinsbergen, D. J. (2022). On pole position: Causes of dispersion of the paleomagnetic poles behind apparent polar wander paths. *Journal of Geophysical Research: Solid Earth*, *127*(4), e2022JB023953. <https://doi.org/10.1029/2022jb023953>
- Vaes, B., Li, S., Langereis, C. G., & van Hinsbergen, D. J. (2021). Reliability of palaeomagnetic poles from sedimentary rocks. *Geophysical Journal International*, *225*(2), 1281–1303. <https://doi.org/10.1093/gji/ggab016>
- Vaes, B., van Hinsbergen, D., & Paridaens, J. (2024). APWP-online.org: A global reference database and open-source tools for calculating apparent polar wander paths and relative paleomagnetic displacements. *tektonika*, *2*(1), 174–189. <https://doi.org/10.55575/tektonika2024.2.1.44>
- Vaes, B., van Hinsbergen, D. J., & Boschman, L. M. (2019). Reconstruction of subduction and back-arc spreading in the NW Pacific and Aleutian Basin: Clues to causes of Cretaceous and Eocene plate reorganizations. *Tectonics*, *38*(4), 1367–1413. <https://doi.org/10.1029/2018tc005164>
- Vaes, B., van Hinsbergen, D. J., van de Lagemaat, S. H., van der Wiel, E., Lom, N., Advokaat, E. L., et al. (2023). A global apparent polar wander path for the last 320 Ma calculated from site-level paleomagnetic data. *Earth-Science Reviews*, *245*, 104547. <https://doi.org/10.1016/j.earscirev.2023.104547>
- Van der Meer, D. G., van Hinsbergen, D. J., & Spakman, W. (2018). Atlas of the underworld: Slab remnants in the mantle, their sinking history, and a new outlook on lower mantle viscosity. *Tectonophysics*, *723*, 309–448. <https://doi.org/10.1016/j.tecto.2017.10.004>
- Van der Wiel, E., van Hinsbergen, D. J., Thieulot, C., & Spakman, W. (2024). Linking rates of slab sinking to long-term lower mantle flow and mixing. *Earth and Planetary Science Letters*, *625*, 118471. <https://doi.org/10.1016/j.epsl.2023.118471>
- Van Hinsbergen, D. J., Torsvik, T. H., Schmid, S. M., Mañenco, L. C., Maffione, M., Vissers, R. L., et al. (2020). Orogenic architecture of the Mediterranean region and kinematic reconstruction of its tectonic evolution since the Triassic. *Gondwana Research*, *81*, 79–229. <https://doi.org/10.1016/j.gr.2019.07.009>
- Wang, C., Gordon, R. G., Zhang, T., & Zheng, L. (2019). Observational test of the global moving hot spot reference frame. *Geophysical Research Letters*, *46*(14), 8031–8038. <https://doi.org/10.1029/2019gl083663>
- Wang, C., & Mitchell, R. N. (2023). True polar wander in the Earth system. *Science China Earth Sciences*, *66*(6), 1165–1184. <https://doi.org/10.1007/s11430-022-1105-2>
- Wilson, J. T. (1963). A possible origin of the Hawaiian Islands. *Canadian Journal of Physics*, *41*(6), 863–870. <https://doi.org/10.1139/p63-094>

- Woodworth, D., & Gordon, R. G. (2018). Paleolatitude of the Hawaiian hot spot since 48 Ma: Evidence for a mid-Cenozoic true polar stillstand followed by late Cenozoic true polar wander coincident with Northern Hemisphere glaciation. *Geophysical Research Letters*, *45*(21), 11–632. <https://doi.org/10.1029/2018gl080787>
- Yi, Z., Liu, Y., & Meert, J. G. (2019). A true polar wander trigger for the great Jurassic east Asian Aridification. *Geology*, *47*(12), 1112–1116. <https://doi.org/10.1130/g46641.1>